International Journal of Heat and Mass Transfer 102 (2016) 645–656

Contents lists available at ScienceDirect

International Journal of Heat and Mass Transfer

journal homepage: www.elsevier.com/locate/ijhmt

Numerical study of vertical solar chimneys with moist air in a hot and humid climate

Sudaporn Sudprasert [a,*], Chatchawin Chinsorranant [a], Phadungsak Rattanadecho [b]

[a] Faculty of Architecture and Planning (Building Technology), Thammasat University, 99 Mu 18 Klongluang, Patumthani, Thailand
[b] Center of Excellence in Electromagnetic Energy Utilization in Engineering (CEEE), Department of Mechanical Engineering, Thammasat University, 99 Mu 18 Klongluang, Patumthani, Thailand

ARTICLE INFO

Article history:
Received 24 November 2015
Received in revised form 16 June 2016
Accepted 18 June 2016

Keywords:
Solar chimney
Moist air
Natural ventilation
CFD
Hot and humid
Species transport

ABSTRACT

The purpose of this study was to investigate numerically the effect of moist air on the performance of a vertical solar chimney. Numerical models were constructed to simulate the heat transfer and fluid flow of dry air and moist air with a relative humidity of 30–80% in a solar chimney. Computational results of air velocity and temperature distribution in the solar chimney with dry air were compared to results with moist air, under a constant chimney wall temperature. Compared to a solar chimney with dry air, the yield of ventilated air flow was 15.4–26.2% less and the overall air temperature was higher for a solar chimney with moist air. To maximize ventilation and reduce backward flow at the opening, an aspect ratio of 14:1 and a limited opening height are recommended for solar chimneys with moist air.

1. Introduction

There have been many investigations of the thermal performances of variously designed solar chimneys integrated with buildings. Although invented for use in heating and ventilation applications in a cold climate [1] the solar chimney has been studied and applied under various climatic conditions. The thermal performance, in terms of the volume flow rate, air velocity, and air temperature, depends on the chimney configuration, construction materials, and integrated renewable energy systems [2].

The amount of water vapor in the air is dissimilar in different climates. For example, one study in a hot-dry climate reported a mean ambient temperature in the summer of 30–34 °C and relative humidity (RH) of less than 20% [3]. Another study in a hot–humid climate reported an ambient summertime temperature of 33.4–37.5 °C and RH of 46.0–73.5% [4]. The water content of air was greater in the hot–humid compared to the hot-dry climate by around 10 grams of moisture per kilogram of dry air. In a hot–humid climate, high vapor content in the air will affect the thermal performance of a solar chimney and lead to specific design specifications. Specifically, air flowing inside a solar chimney in a hot–humid climate could behave like moist air, or a mixture of water vapor and dry air.

Studies have covered diverse areas related to the volume flow rate of solar chimneys of various configurations. In India, for example, experiments showed results of 2.4–5.6 air change per hour (ACH) for an absorber area of 0.7–0.9 m^2 [5]. In the hot–dry climate of Iraq, a solar chimney with an incline of 60°, aspect ratio of 13.3, and chimney length of 2 m gave 4–35 ACH for an inflow velocity of 0.3–0.8 m/s [6]. A vertical solar chimney integrated with a water spraying system in Iran [3] gave an average of 4.51–8.28 ACH for an average velocity of 0.2–0.3 m/s. The room temperature approached a comfortable temperature with an indoor RH of 10.7–34.3%. The outdoor RH did not have a significant effect on the air velocity inside the channel.

There have not been many studies of the effects of humidity on solar chimneys in hot–humid climates because the humidity is not considered to have a primary effect on the ventilation. Ventilation performance has been determined by combining the wall and the roof [7], changing the configuration [8] and [9], increasing the inclination angle [3], and increasing the temperature difference between the inlet and outlet [10] and [11] of the solar chimney. Application of direct evaporation has been avoided in hot–humid climates. Only one experiment of an inclined solar chimney with indirect evaporative cooling was found [4], which was performed in Thailand. Solar chimney is used to drive the warm air inside it to rise along the wall, which can be used for building ventilation,

* Corresponding author.
E-mail address: sudaporn@ap.tu.ac.th (S. Sudprasert).

http://dx.doi.org/10.1016/j.ijheatmasstransfer.2016.06.054
0017-9310/

Nomenclature

c_p	specific heat (J/kg·K)
$D_{i,m}$	mass diffusion coefficient for species i in the mixture (m^2/s)
$D_{i,T}$	thermal diffusion coefficient for species i in the mixture (m^2/s)
g_i	gravitational acceleration in the i direction (m/s^2)
H	height of air gap (m)
h	height of opening (m)
J_i	mass diffusion ($kg/s·m^2$)
k	thermal conductivity (W/m·K)
L	width of air gap (m)
P	static pressure (Pa)
P_{atm}	atmospheric pressure (Pa)
Sc_t	turbulent Schmidt number
t	time (s)
T	time-mean temperature of fluid (°C)
T'	fluctuation temperature (°C)
T_0	reference temperature (=31.0 °C)
T_{w1}	temperature of air contacting the hot surface (°C)
T_{w2}	temperature of air contacting the cold surface (°C)
$T_{\alpha 1}$	ambient temperature (°C)
$T_{\alpha 2}$	air temperature at the inlet (°C)
u_i	mean velocity component corresponding to i direction (m/s)
u'_i	fluctuation velocity component in the i direction (m/s)
x_i	coordinate direction i (m)
Y_i	local mass fraction of each species

Greek symbols

β	coefficient of thermal expansion ($=1/T_0$) (1/K)
ρ	density of fluid (kg/m^3)
μ	laminar dynamic viscosity (kg/m·s)
υ	kinematic viscosity (m^2/s)
γ	diffusion coefficient

power generation, drying, etc. The solar chimney for building ventilation is similar to the solar updraft tower (also called solar chimney) for power generation [12]. In a solar updraft power plant where the buoyancy effect was applied to drive the wind turbine, under high relative humidity, the power generation became smooth, power was increased, and condensation was observed [13].

In the design of solar chimney configurations, the commercial CFD software has been widely used to determine the proper height to width ratio of the air gap [14] and the inlet positions [15] to maximize the mass flow rate. The height of the air gap (H), width of the air gap (L), and height of the opening (h) affected the ventilation rate of the solar chimney. A numerical study showed that the optimal aspect ratio varied with the Raleigh number (Ra_L) under uniform heat flux and uniform wall temperature [16]. On the basis of computational results, Gan (2006) recommended an air–gap height to width ratio (H/L) of 11.11 or 20.0. A wall solar chimney in Thailand showed the highest volume flow rate with H/L = 14 [17].

The purpose of the present study was to compare the air flow and temperature distributions within a vertical solar chimney when using moist air compared to dry air. Here, moist air refers to air with a range of RH typical of Thailand (RH = 40–80%). The air velocity and temperature distribution of moist air in the air gap were obtained simultaneously by using the computational software ANSYS Fluent 14.0. Results obtained from moist air simulated by the species transport model were compared to results from the dry-air model. Effects of moist air on the solar chimney aspect ratio and inlet height were also studied.

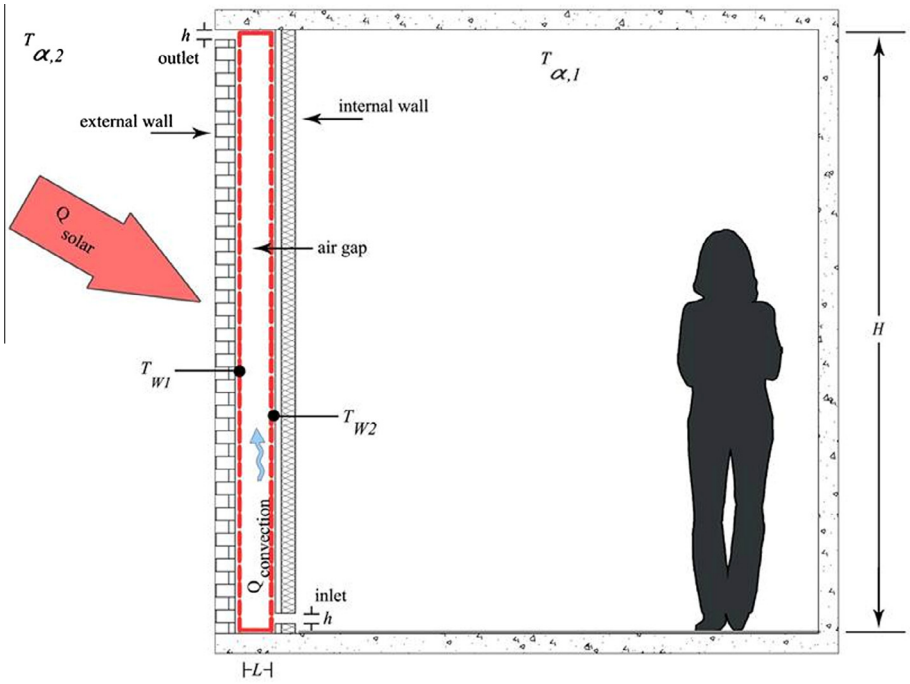

Fig. 1. Air gap of the solar chimney subjected to constant surface temperatures.

Table 1
Temperatures (°C) of solar chimney wall and air gap [17].

Time	Surface W1 (T_{w1})	Surface W2 (T_{w2})	Air in middle (T_a)	Inlet air
16.00	32.28	29.00	31.20	30.80
16.15	32.38	28.79	30.90	27.40
16.30	32.10	28.91	31.20	30.10
16.45	32.38	29.03	31.00	30.70
17.00	32.35	29.09	30.90	27.50

Table 2
Mass fractions of inflow air-vapor mixture.

Relative humidity (%)	Vapor	Dry air
–	0	1.000
40	0.010	0.990
50	0.013	0.987
70	0.019	0.981
80	0.023	0.977

Table 3
Thermal properties of air and vapor at operating temperature [20].

Properties	Unit	Air	Vapor
k	W/mK	0.02588	0.01896
c_p	J/kgK	1007	1874
ρ	kg/m^3	1.164	0.723
υ	m^2/s	1.872×10^{-5}	1.407×10^{-5}

Table 4
Average velocity at the openings of the dry air and air-vapor mixture models.

Relative humidity (RH, %)	Average air velocity (m/s)		Difference from dry air (%)	
	Inlet	Outlet	Inlet	Outlet
Dry air	0.0550	0.0693	–	–
40	0.0408	0.0586	25.8	15.4
50	0.0407	0.0586	26.0	15.4
70	0.0407	0.0585	26.0	15.6
80	0.0406	0.0585	26.2	15.6

2. Problem formulation and numerical modeling

Fig. 1 depicts the physical configuration of a two-dimensional (2-D) air gap of a vertical solar chimney. In this study, the solar induced ventilation is assumed mainly effect across the inlet and outlet openings placed on the right and the left walls, respectively. This assumption is valid when the widths of inlet and outlet openings are identical to the width of the walls and the measurement of air temperature and velocity are conducted at the middle section of the wall. According to the control volume of the solar chimney reported in previous studies [17,18], a 2-D air gap in a solar chimney with an H/L ratio of 14:1 was used (Fig. 1). The height of the inlet and outlet openings was 0.05 m. The surface temperature of the solar chimney was slightly different from that in previous studies [17,18]. Surface temperature along the vertical walls was assumed to be constant and equal to T_{w1} and T_{w2} along the external and internal wall, respectively. The upper roof and bottom walls were assumed to be adiabatic. The bottom inlet was subjected to room air ($T_{\alpha 2}$), and the top outlet was exposed to ambient air ($T_{\alpha 1}$).

Due to the buoyancy effect contributed by heat accumulated on the external wall, warm air in the air gap was discharged to the ambient air via the outlet at the top of the external wall. Then, room air was drawn into the air gap through the inlet opening at the bottom of the internal wall, creating natural ventilation in the adjacent room. The constant surface temperatures were taken from previous research [17], as shown in Table 1. Data were averaged every 15 min for 1 h between 4 and 5 p.m. in a solar chimney installed in the west end of a testing room. The wall temperatures were steady, while the air temperature at the inlet varied from 27.4 to 30.4 °C, during the hour (Table 1).

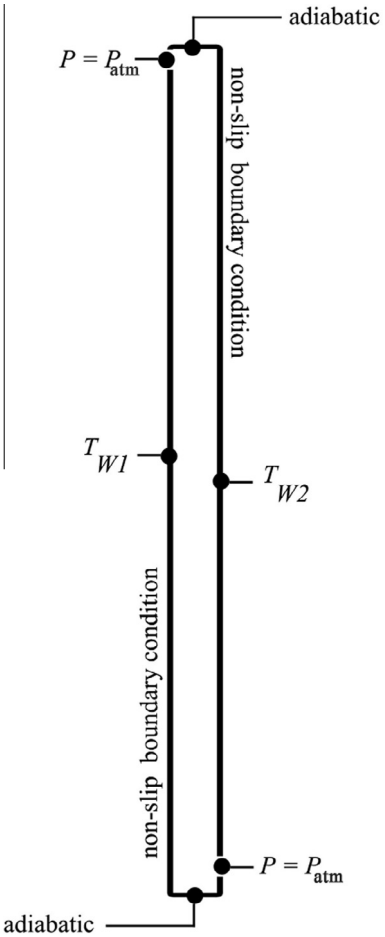

Fig. 2. Boundary conditions for analysis of heat transfer and fluid flow.

As the present work was mainly concerned with the effects of moist air on the volume flow rate and aspect ratio of the solar chimney, dry and moist air were the two working fluids studied in solar chimneys of similar configurations. The dry-air model employed the air property of an ideal gas. Moist air was simulated as an air-vapor mixture using the species transport model [19]. Mass fractions of the air-vapor mixture corresponding to RH = 40–80% are shown in Table 2. Thermal properties of the air and vapor at an operating temperature of 30.5 °C are shown in Table 3. Under the moist-air condition, solar chimney aspect ratios of 30:1, 14:1, and 10:1 were considered. Ratios of the opening height to the solar chimney width (h/L) of 0.25, 0.50, and 0.75 were examined in the solar chimney with an aspect ratio of 14:1.

To analyze the numerical CFD models of dry and moist air, the problem was simplified by assuming constant thermal properties of air and vapor. Air flow in the air gap was assumed to be turbulent, and the k–ε Re-Normalisation Group (RNG) turbulence model was used to simulate the effect of turbulence. The difference in air temperatures between the inlet and outlet of the solar chimney was not high, and the Boussinesq approximation was employed in the dry air model.

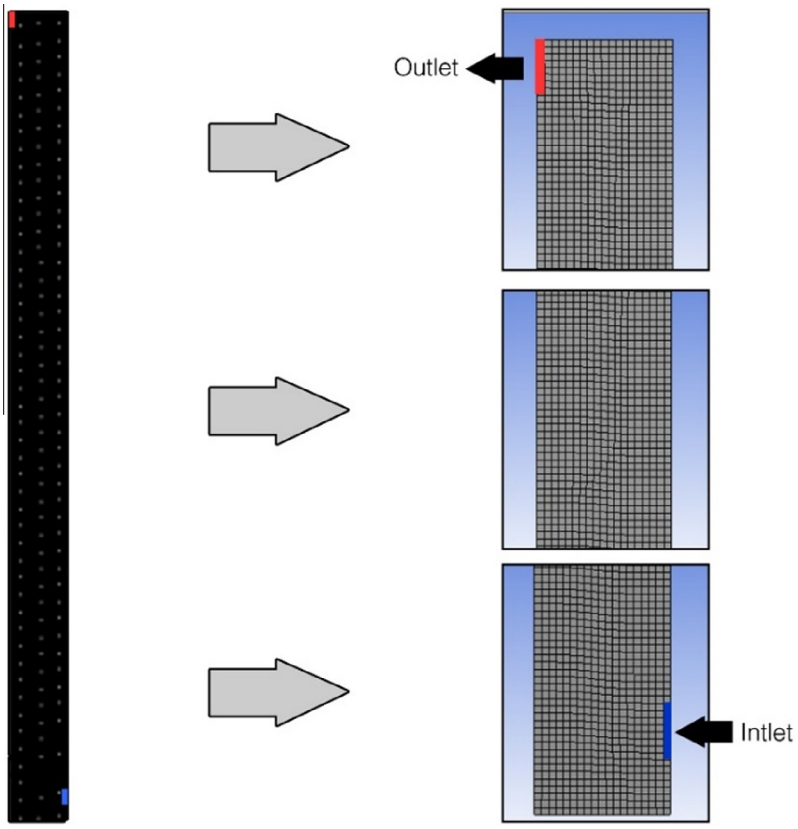

Fig. 3. A two-dimensional finite volume grid of the air gap in solar chimney.

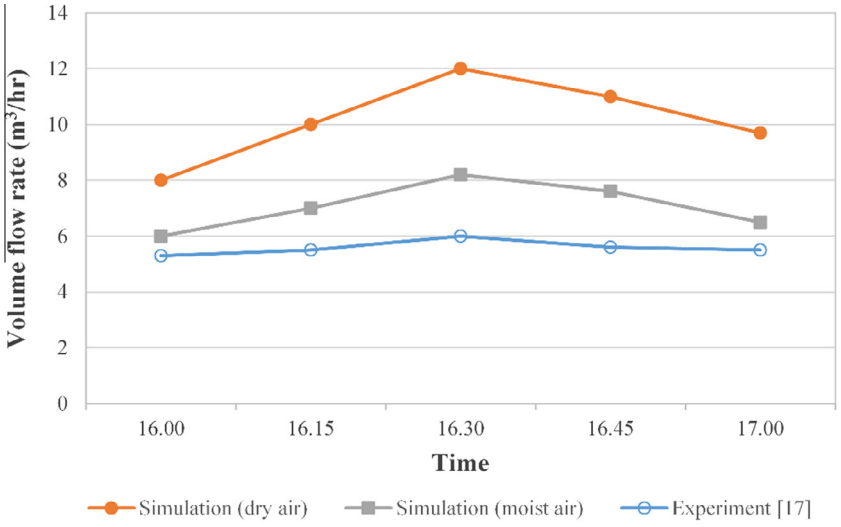

Fig. 4. Comparison of numerical and experimental results of volume flow rates.

In the simulation of moist air, the water vapor had no reaction and no phase change. Moist air was assumed to be a mixture of water vapor (H_2O) and gas (O_2, N_2) molecules. Thus, the species transport model was used to compute air velocity and temperature distribution from the input properties of the air-vapor mixture. Under this assumption, the governing equations can be solved for a 2-D transient turbulent flow, as follows [21]:

Continuity equation:

$$\frac{\partial \rho}{\partial t} + \frac{\partial}{\partial x_i}(\rho u_i) = 0 \tag{1}$$

Momentum equation:

$$\frac{\partial}{\partial t}(\rho u_i) + \rho u_j \frac{\partial u_i}{\partial x_j} = -\frac{\partial P}{\partial x_i} + \frac{\partial}{\partial x_j}\left(\mu \frac{\partial u_i}{\partial x_j} - \rho \overline{u_i u_j}\right) + \rho g_i \beta (T - T_0) \tag{2}$$

Energy equation:

$$\frac{\partial}{\partial t}(\rho T) + \rho u_j \frac{\partial T}{\partial x_j} = \frac{\partial}{\partial x_j}\left(\gamma \frac{\partial T}{\partial x_j} - \rho \overline{u_j' T'}\right) \tag{3}$$

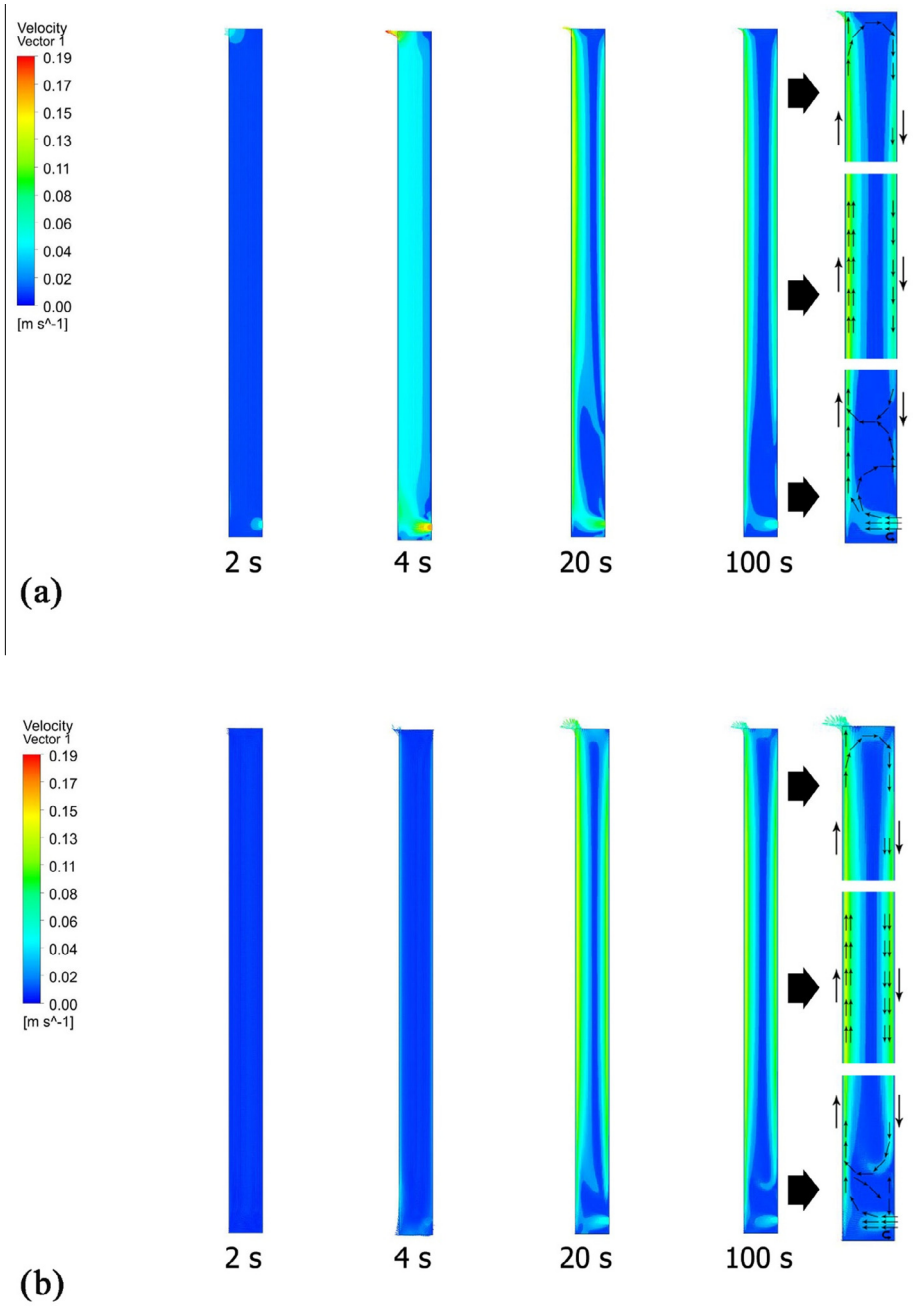

Fig. 5. The transient simulation results of air velocity in the solar chimney with (a) dry air and (b) moist air.

For all flows, the ANSYS Fluent program was used to solve the conservation equations for mass (Eq. (1)) and momentum (Eq. (2)). For flow involving heat transfer, an additional equation for energy conservation (Eq. (3)) was solved. For flows involving a mixture of species, the species conservation equation was solved. To solve conservation equations for species, the ANSYS Fluent software predicts the local mass fraction of each species, Y_i, through solution of a convection–diffusion equation for the ith species. This conservation equation takes the following form:

$$\frac{\partial}{\partial t}(\rho Y_i) + \nabla \cdot (\rho u_i Y_i) = -\nabla \cdot J_i \tag{4}$$

There are two species in the CFD model: water vapor (species 1) and air (species 2). In turbulent flow, ANSYS Fluent computes the mass diffusion in the following form:

$$J_i = -\left(\rho D_{i,m} + \frac{\mu_t}{Sc_t}\right)\nabla Y_i - D_{i,T}\frac{\nabla T}{T} \tag{5}$$

2.1. Boundary conditions

Boundary conditions needed to solve the governing equations are shown in Fig. 2. Air contacting the external or internal wall was considered to have a boundary condition of constant temperature T_{w1} or T_{w2}, respectively. The top wall (#3) and bottom wall (#4) were assumed to be adiabatic. Boundary conditions for solving the momentum equation were no-slip at the boundaries and atmospheric pressure at the openings.

2.2. Calculation procedures

Navier–Stokes and energy equations with boundary condition Eqs. (11)–(15) were solved by using the computational fluid dynamic code ANSYS Fluent. Convective terms in the governing equations for momentum, turbulent kinetic energy, turbulent dissipation rate, and energy were discretized with the second-order

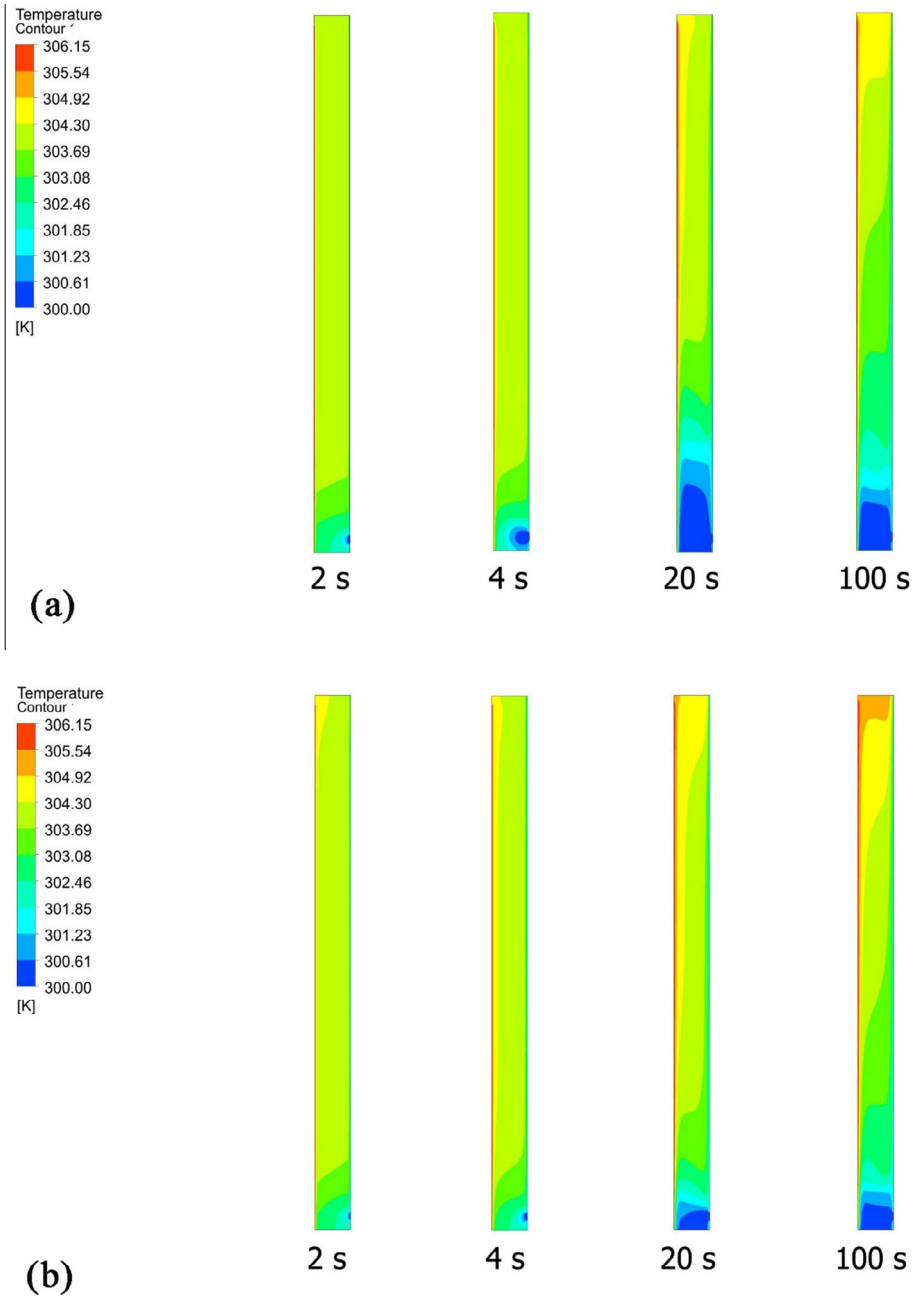

Fig. 6. The transient simulation results of air temperature in the solar chimney with (a) dry air and (b) moist air.

upwind scheme. PRESTO! was used as the pressure interpolation scheme because the solar chimney has natural convective flow with a high Rayleigh number. Coupling between velocity and pressure was performed with the SIMPLE algorithm.

Convergence of the numerical solution was considered to have been achieved when the sum of the normalized residuals for each flow equation was less than 10^{-4}. The convergence test was conducted to identify the appropriate number of grids required. To validate the independence of the solution on the grid, four node numbers (4100, 6400, 11,200 and 24,700) were investigated. Simulation results showed that the temperature distribution and velocity vectors were similar with node numbers of 11,200 and 24,700. Hence, the model with 11,200 nodes was selected for further studies. Fig. 3 shows the results of the uniform grids in the solar chimney.

3. Validation of numerical results

Apart from the investigations of grid independency, the heat transfer and fluid flow characteristics were compared with available experimental results. To validate the reliability of the numerical method being used, the numerical simulation was conducted with the solar chimney with the same geometrical configuration as presented in [17]. Dry and moist air are the working fluids in the simulation models. Temperature values at the wall boundaries and inlet in the simulation models followed the experimental results in Table 1.

Fig. 4 shows the numerical and experimental results of the volume flow rate after 1 h of operation. The volume flow rate from the simulation results of the dry-air model were very different from the experimental results. Simulation results of the moist-air model

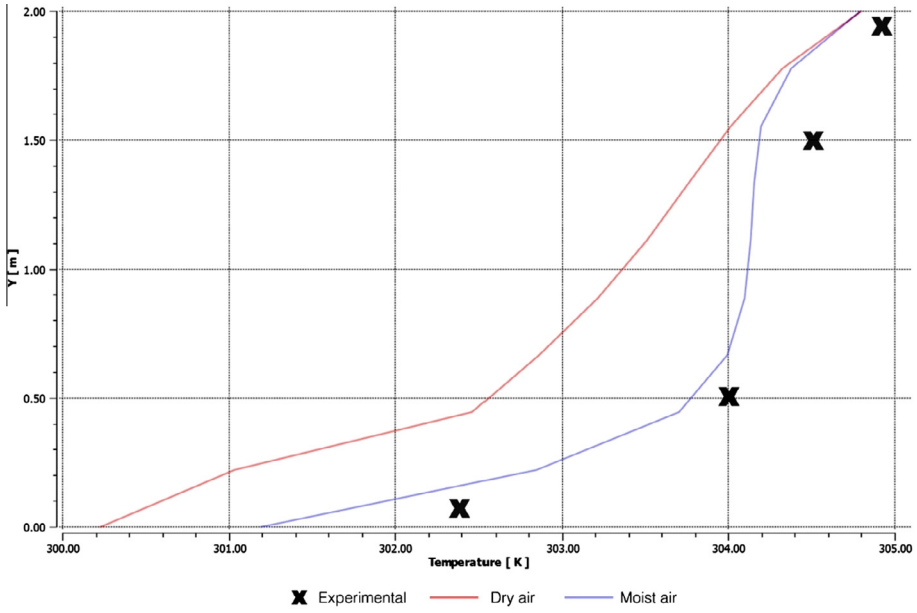

Fig. 7. Temperature profile along the air gap height.

agreed well with experiment results, with a difference of 20–33%. This difference was still high because the results obtained from the 2-D model limit the prediction of the experimental results. The local speed computed at some points may not be real. However, the comparison showed that using the species transport model for the computational modeling of moist air can improve the calculation of volume flow rate through the solar chimney.

4. Results and discussion

The following sections present the numerical results obtained from the 2-D model shown in Fig. 2. The transient simulations approached the steady state at 100 s. Simulations were carried out under a hot wall temperature of T_{w1} = 33 °C and cool wall temperature of T_{w2} = 29 °C. Computational results of air velocity and temperature distribution in the air gap were analyzed through graphical displays produced by the CFD package. Ventilation performances of the solar chimney with different water vapor contents are presented in terms of the volume flow rate.

4.1. Air velocity in the solar chimney with the dry- and moist-air models

Fig. 5 shows the transient simulation results of air velocity in the air gap of the solar chimney with dry or moist air. The dry-air model (Fig. 5a) depicted air close to the hot surface flowing upward from the inlet due to the buoyancy effect, starting from 2 s until 100 s. A portion of the air left the air gap through the outlet, while another portion of air turned back to the cool surface. The backward air flowed down to 0.44 m above the inlet opening and flowed up again close to the hot surface. This recirculation around the borders of the air gap created a region of zero air velocity at the center of the air gap.

In the moist-air model with RH = 70% (Fig. 5b), warm air started moving at 10 s. The flow characteristics were similar to those of the dry-air model. However, the portion of air that turned back was larger in the moist-air model, and the volume of this moist air fell to 0.13 m above the inlet opening. Images on the right-hand side in Fig. 5a and b show the magnification of velocity vectors in the solar chimney at 100 s for the dry- and moist-air models, respectively. There was greater mixing of the room air entering the inlet with the warm recirculation stream in the moist- compared to the dry-air model. Because the disturbance at the inlet was less, dry air flowed into the solar chimney at higher velocity than the moist air.

4.2. Effect of vapor content on air velocity

An increase in RH at a constant mixture temperature involves an increase of the vapor mass fraction in the air-vapor mixture. Increasing the vapor in the mixture by increasing the RH from 40% to 80% reduced the average velocity in the solar chimney (see Table 4). Compared to the results of the dry model, the air-vapor mixture model with RH = 80% delivered 15.6% lower air velocity at the exit. The vapor density was smaller than that of the dry air, resulting in the reduction of buoyancy in the moist-air model. In addition, vapor required higher heat to increase the temperature by 1 °C, due to its higher specific heat compared to dry air of the same mass. Overall, the buoyancy force decreased when vapor was considered in the computational model.

4.3. Temperature distribution in the solar chimney with dry- and moist-air models

Fig. 6 shows the numerical results of air temperature in the solar chimney with the dry- (Fig. 6a) or moist-air model (Fig. 6b). The air temperature was distributed from 300 to 306 K in the dry-air model, with an average air temperature in the air gap of 303.46 K (30.46 °C). Fig. 6b shows the results of the air temperature obtained from the moist-air model with RH = 70%. The temperature distribution was similar for RHs of 40% to 80%. The average air temperature in the moist-air model was 303.96 K (30.96 °C), which is slightly higher than the average temperature in the dry-air model.

The temperature range in the moist-air model was higher than that of the dry-air model, which can be explained by the delayed and reduced discharging of air. Heat quickly dissipated in the air gap, and the temperature increased in the first 2 to 4 s because of the static moist air. At steady state (100 s), the bottom of the air gap with dry air became cool at the inflow air temperature.

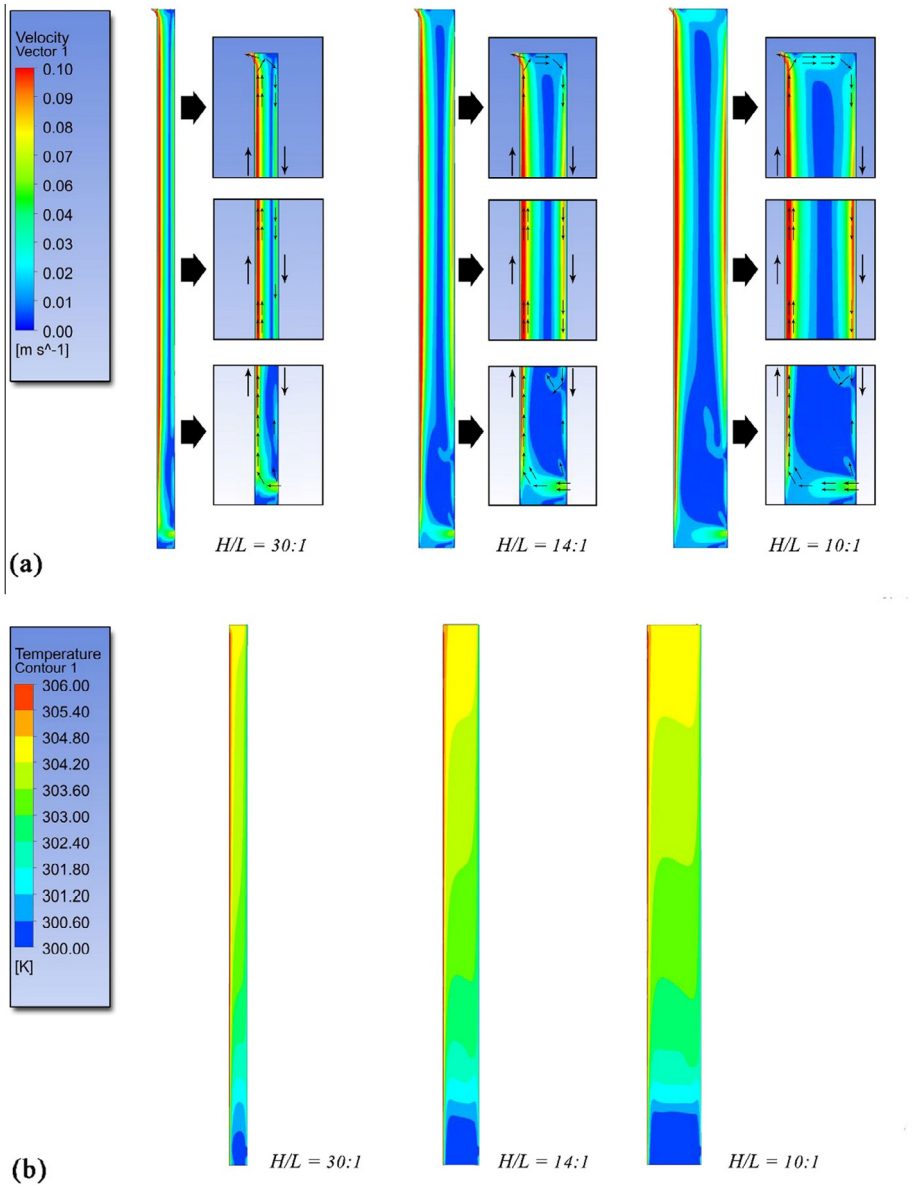

Fig. 8. Simulation results of dry air with aspect ratios of 30:1, 14:1 and 10:1, (a) air velocity and (b) temperature distribution in steady state.

The inlet moist air mixed with the recirculated warm air, and the temperature at the bottom of air gap increased.

Fig. 7 shows the temperature profile along the air–gap height. The dry- and moist-air models had identical temperature profiles; however, the air temperature in the moist-air model was higher than in the dry-air model at equivalent heights in the solar chimney. Compared to experimental research in a hot–humid climate, the moist-air model is more accurate in the prediction of air temperature in the air gap.

4.4. Effect of the aspect ratio

Effects of aspect ratios (H/L) of 30:1, 14:1, and 10:1 (L = 0.1, 0.2, and 0.3 m, respectively, for H = 3.0 m) on the performance of the solar chimney were investigated and compared for the dry- and moist-air models. Fig. 8 shows the simulation results of air velocity (Fig. 8a) and temperature (Fig. 8b) at steady state for the dry-air model. The directions of flow and recirculating air were similar at all three aspect ratios, except for backward flow at the outlet opening with the largest air gap. The largest air gap has a larger portion of backward airflow than the smallest air gap. For L = 0.1, 0.2, and 0.3 m, dry air flowed into the air gap through the inlet and exited through the outlet. Air temperatures at the three aspect ratios were stratified, with a low temperature at the bottom and high temperature at the top of the air gap.

Fig. 9 shows the simulation results for the moist-air model in a solar chimney with different aspect ratios. For a solar chimney with an air–gap width of 0.1 or 0.3 m, two regions of air recirculation separated by static air developed in the steady-state condition (Fig. 9a). Outflow involved only warm air that had collected near the outlet, and excluded the stream of inflow air. Furthermore, reverse flows were found at the inlet. The flow of moist air was clearly inefficient in the air gap with the incorrect aspect ratios. The nonuniformity of air velocity in the air gap led to a variation in temperature distribution (Fig. 9b). The aspect ratio of 14:1,

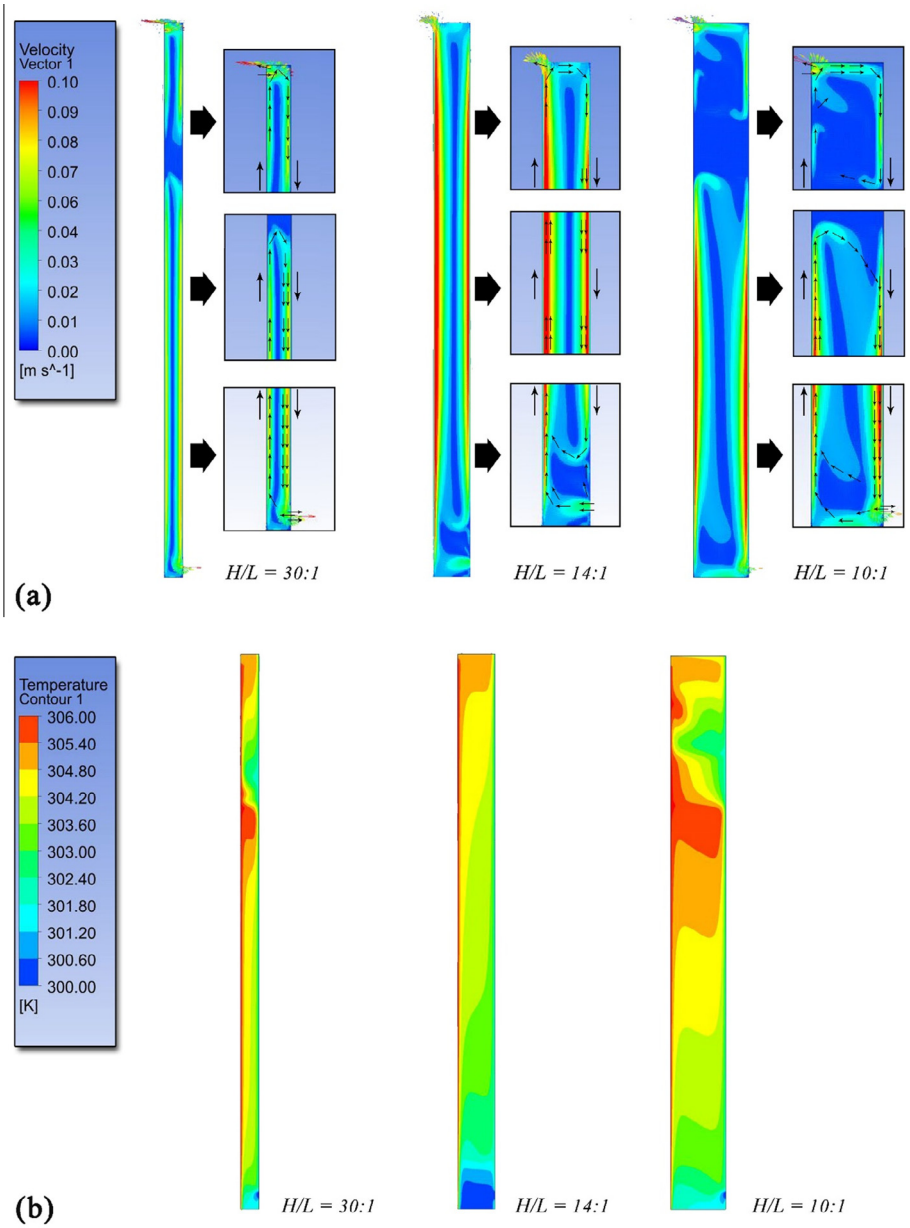

Fig. 9. Simulation results of moist air with aspect ratios of 30:1, 14:1 and 10:1, (a) air velocity and (b) temperature distribution in steady state.

reported in Refs. [17,18] was verified to be appropriate for moist-air application in this study.

4.5. Effect of the height of the opening

Heights of the inlet and outlet openings were varied to study their effect on the ventilation performance of the solar chimney. The recommended opening height was 0.05 m ($h/L = 0.25$) for the inlet and outlet. Simulation results showed the detailed thermal behavior of the dry and moist air. The h/L ratios of 0.25, 0.50, and 0.75 were created for an air gap with a height of 3 m and width of 0.2 m.

Fig. 10 shows the computational results of air velocity (Fig. 10a) at steady state and air temperature (Fig. 10b) for dry air in the air gap. Changing the inlet and outlet opening heights in the dry-air model did not alter the flow pattern or temperature distribution in the air gap. Reverse flow at the inlet and outlet openings was found in the air gap with a large opening ($h/L = 0.50$ and 0.75). The air temperature in the air gap was almost identical for all three h/L ratios, except that reverse flow produced a high temperature at the outlet.

Fig. 11 shows the simulation results obtained from the analysis of moist air in the air gap of the solar chimney with three opening heights. Changing the opening height of the inlet and outlet had different effects on the air gap. Very large openings reduced the upward flow (Fig. 11a), decreasing the magnitude of the upward velocity while increasing the size of static air region, especially for air gaps with $h/L = 0.5$ or 0.75. Reverse flows were found at the inlet and outlet openings. In other words, ambient air entered the air gap through the outlet, and air in the air gap flowed into the room. Nonuniformity of the air flow was also reflected in the temperature distribution (Fig. 11b). High air temperature was found at the middle of the air gap height because of the backward flow. Therefore, the opening

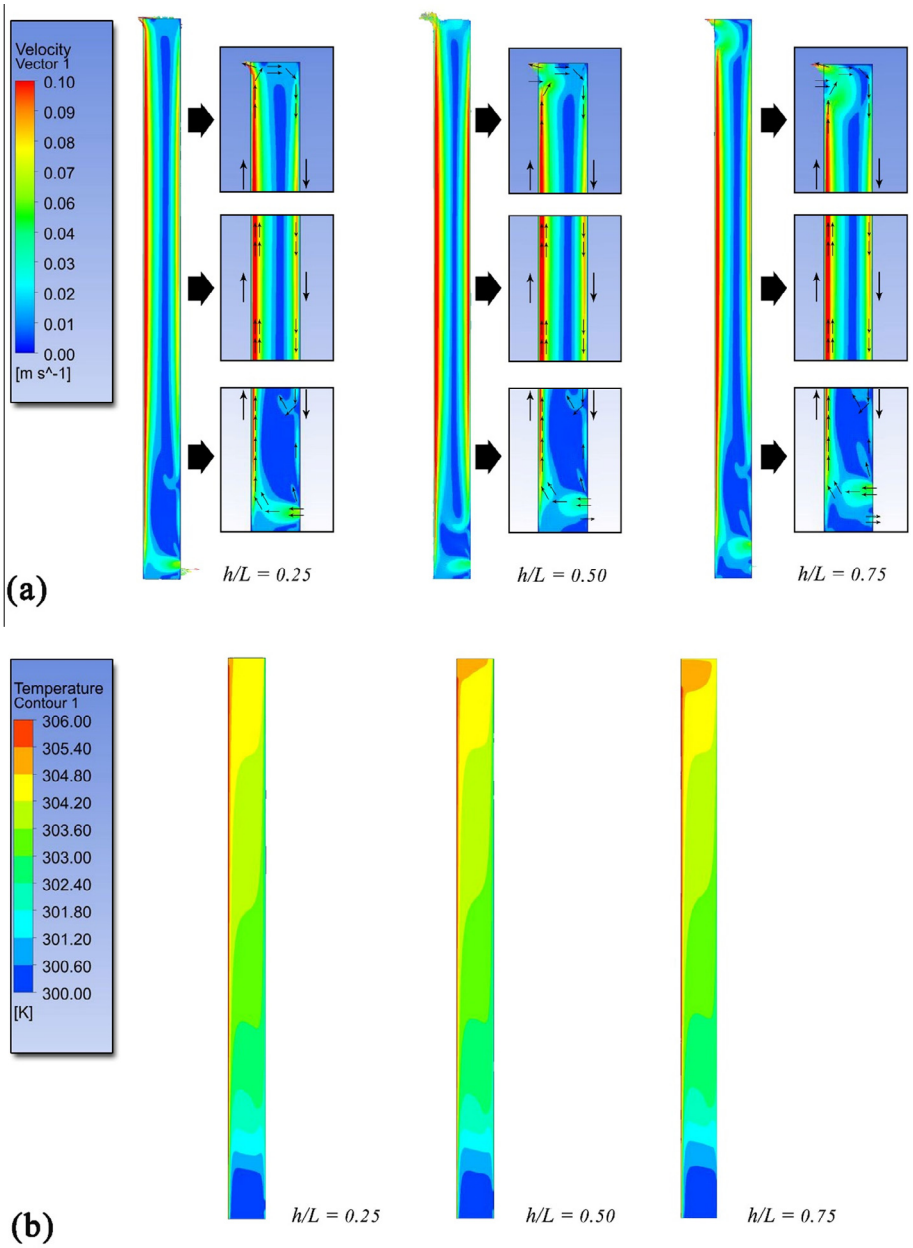

Fig. 10. Computational results of (a) velocity and (b) temperature in steady state of dry air in the air gap with h/L ratios of 0.25, 0.50 and 0.75.

height should be limited to $h/L = 0.25$ for application of a solar chimney with moist or dry air, to avoid reverse flow.

5. Conclusions

This study investigated the effects of the vapor mass fraction in the air-vapor mixture on the temperature distribution and velocity flow patterns in the air gap of a solar chimney. Effects of increasing the RH at a constant temperature on the air temperature distribution and airflow were ascertained by numerically simulating transport models of heat transfer and species conservation. The air temperature distribution was directly influenced by the amount of water vapor in the air. Increasing the vapor mass fraction of the air-vapor mixture reduced the air velocity at the inlet and outlet openings by 26% and 15.6%, respectively, compared to dry air under the same boundary conditions. Furthermore, increasing the vapor mass fraction intensified the recirculation of warm air near the openings and reduced the ventilation through the air gap. The air temperature distribution in the air-vapor mixture model developed similarly to the temperature distribution in the dry-air model, but with a slightly higher air temperature.

From these results, we conclude that the water vapor should be considered in the application of a solar chimney in a hot–humid environment. The suggested aspect ratio (H/L) of 14:1 was verified with the air-vapor mixture simulation model. To increase the upward flow and prevent backward flow into the room, small opening heights, such as $h/L = 0.25$, are recommended for solar chimneys used with moist air.

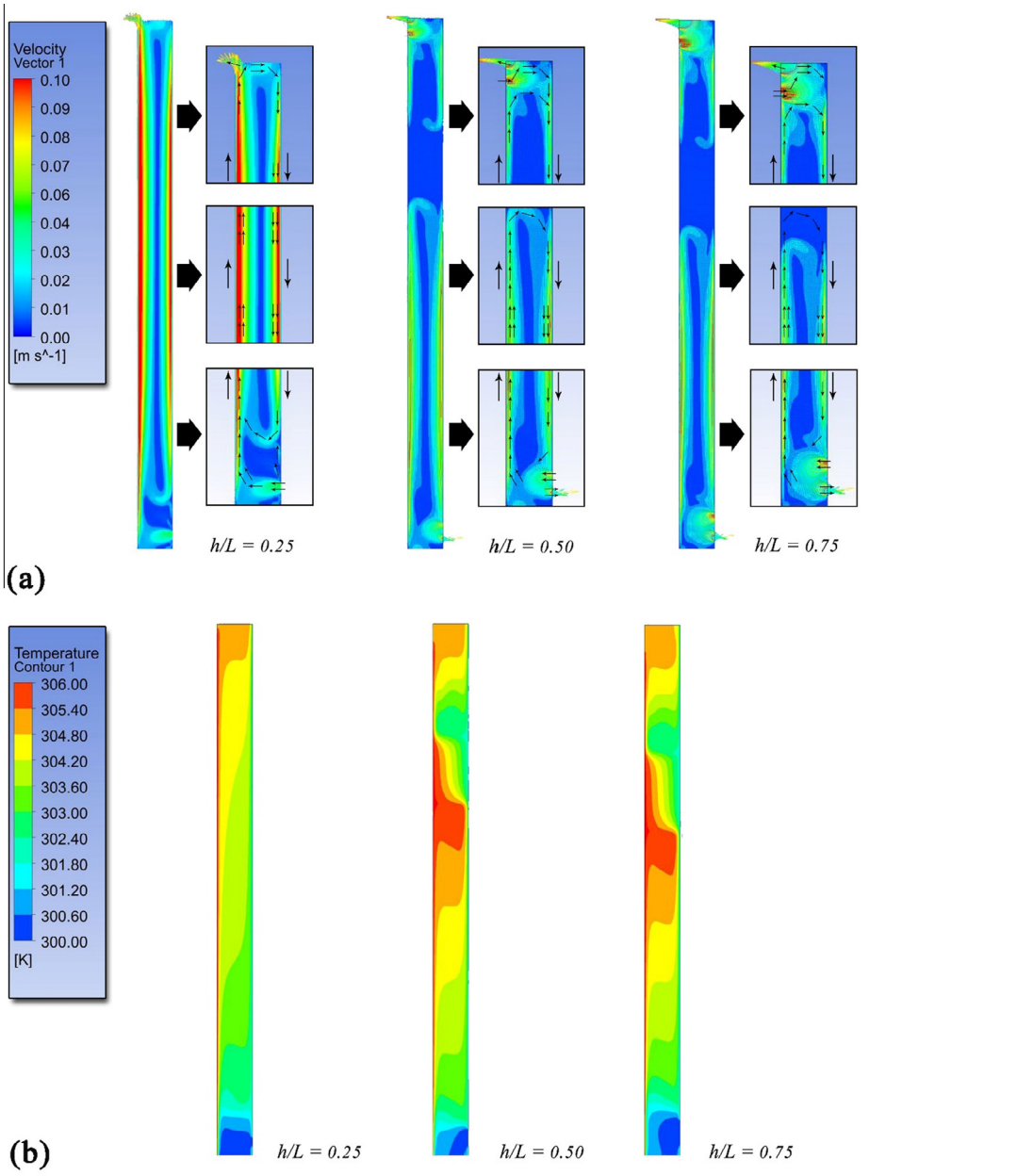

Fig. 11. Computational results of (a) velocity and (b) temperature in steady state of moist air in the air gap with h/L ratios of 0.25, 0.50 and 0.75.

Acknowledgements

The authors gratefully acknowledge the financial support provided by the Thammasat University Research Fund under Research Scholar Contract No. 55/2558, the Thailand Research Fund under TRF Contract Nos. RTA5680007 and TRG5780255, and the National Research Universities Project of Higher Education Commission for supporting this research.

References

[1] O. Saadatian, K. Sopian, C.H. Lim, N. Asim, M.Y. Sulaiman, Trombe wall: a review of opportunities and challenges in research and development, Renewable Sustainable Energy Rev. 16 (2012) 6340–6351.
[2] X.Q. Zhai, Z.P. Song, R.Z. Wang, A review for the applications of solar chimneys in buildings, Renew. Sustain. Energy Rev. 15 (2011) 3757–3767.
[3] M. Rabani, V. Kalantar, A.A. Dehghan, A.K. Faghih, Empirical investigation of the cooling performance of a new designed trobmbe wall in combination with solar chimney and water spraying system, Energy Build. 102 (2015) 45–57.
[4] S. Chungloo, B. Limmeechokchai, Application of passive cooling systems in the hot and humid climate: the case study of solar chimney and wetted roof in Thailand, Build. Environ. 42 (2007) 3341–3351.
[5] J. Mathur, N.K. Bansal, S. Mathur, M. Jain, Anupma, Experimental investigation on solar chimney for room ventilation, Sol. Energy 89 (2006) 927–935.
[6] A.A. Imran, J.M. Jalil, S.T. Ahmed, Induced flow for ventilation and cooling by a solar chimney, Renewable Energy 78 (2015) 236–244.
[7] J. Khedari, B. Boonsiri, J. Hirunlabh, Ventilation impact of a solar chimney on indoor temperature fluctuation and air change in a school building, Energy Build. 32 (2000) 89–93.
[8] J. Hirunlabh, S. Wachirapuwadon, N. Pratinthong, J. Khedari, New configuration of a roof solar collector maximizing natural ventilation, Build. Environ. 36 (2001) 383–391.
[9] R. Khanal, C. Lei, A numerical investigation of buoyancy induced turbulent air flow in and inclined passive wall solar chimney for natural ventilation, Energy Build. 93 (2015) 217–226.
[10] G. Gan, S.B. Riffat, A numerical study of solar chimney for natural ventilation of buildings with heat recovery, Appl. Therm. Eng. 18 (1998) 1171–1187.
[11] J. Waewsak, Hirunlabh, J. Khedari, U.C. Shin, Performance evaluation of the BSRC multi-purpose bio-climatic roof, Build. Environ. 38 (2003) 1297–1302.
[12] X. Zhou, Y. Xu, Solar updraft tower power generation, Solar Energy 128 (2016) 95–125.

[13] Y. Xu, X. Zhou, Q. Cheng, Performance of a large scale solar updraft power plant in a moist climate, Int. J. Heat Mass Transfer 91 (2015) 619–629.
[14] G. Gan, Parametric study of trombe walls for passive cooling of buildings, Energy Build. 27 (1998) 37–43.
[15] G. Gan, Simulation of buoyancy-induced flow in opened cavities for natural ventilation, Energy Build. 18 (2006) 410–420.
[16] B. Zamora, A.S. Kaiser, Optimum wall-to-wall spacing in solar chimney shaped channels in natural convection by numerical investigation, Appl. Therm. Eng. 29 (2009) 762–769.
[17] N. Rachapradit, Field study of performance of solar chimney with air-conditioned building Master Thesis in Thermal Technology, King Mongkut's University of Technology Thonburi, Bangkok, 2000.
[18] J. Khedari, C. Lertsatithanakorn, N. Pratinthong, J. Hirunlabh, The modified trombe wall: a simple ventilation means and an efficient insulating materials, Int. J. Ambient Energy (1998) 104–110.
[19] Z. Li, P.K. Heiselberg, CFD Simulations for Water evaporation and Airflow Movement in Swimming Baths, Institute of Bygningsteknik, Aalborg Universitet, 2005.
[20] Y. Cengel, Heat Transfer, McGraw-Hill, Singapore, 2004.
[21] I.N.C. Ansys, ANSYS Fluent Theory Guide, Pennsylvania, USA, 2013.